JOURNAL OF MATERIALS SCIENCE 14 (1979) 1052–1070

Behaviour of an edge dislocation in a semi-infinite solid with surface energy effects

K. JAGANNADHAM, M. J. MARCINKOWSKI
Department of Mechanical Engineering and Engineering Materials Group, University of Maryland, College Park, Maryland 20742, USA

The method of continuously distributed dislocations and the method of discrete distribution of dislocations have been used to determine the effect of surface energy on the surface boundary conditions of a semi-infinite solid containing an edge dislocation. The surface dislocation model which incorporates two surface dislocation arrays, the primary and the secondary, in order of importance, is used to study the effect of surface energy. The surface dislocation model in conjunction with the method of continuously distributed dislocations enables the exact determination of the dislocation distribution function of the primary and secondary dislocation arrays and the effect of surface energy tends to lower both the total Burgers vector associated with the surface arrays and dislocations in evaluating the effect of surface energy is illustrated and is compared with the method of continuously distributed dislocations. It has been found that the surface energy tends to lower both the total Burgers vector associated with the surface arrays and the length of the region within which they are spread on the surface. Although the effect on the primary surface arrays is not very large, the secondary surface arrays are completely eliminated with normal values of surface energy encountered in real solids. Thus, the effect of surface energy is to bring non-vanishing stress components to the surface. The surface is also non-uniformly stressed. The superiority of the surface dislocation model over the other methods hitherto used in the literature is illustrated.

1. Introduction

The elastic properties of a dislocation in an infinite medium have been obtained using the classical theory of elasticity [1, 2]. The elastic properties in a finite medium are obtained when the solutions to the elasticity equations in an infinite medium are modified by the boundary conditions acting on the free surfaces of the finite medium. In the already established methods of linear elasticity, these boundary conditions specify that the stresses acting normal to the free surface should vanish [3]. In the analysis of the elastic properties of a dislocation, various methods are adopted to satisfy the boundary conditions on the surface. The most straightforward, although tedious mathematically, is to solve the elasticity equations. However, there are various short cuts to this method. In the Green's function technique [4], the elasticity equations, for the specific geometry, are already solved to obtain the Green's functions which are the displacements due to a point force. When these are integrated over the cut surfaces forming the dislocation, the boundary conditions are automatically satisfied. Therefore, it is first required to solve the elasticity equations in order to arrive at the Green's functions for the specific geometry.

In the image dislocation model, the surface boundary conditions are satisfied by placing a dislocation of opposite sign in the vacuum, at a distance equal to the position of the dislocation from the free surface. The dislocation in vacuum is called the image dislocation of the real dislocation situated in the homogeneous finite medium [5, 6]. In many cases and even in the simplest situation of an edge dislocation situated in a semi-infinite medium, merely using an image dislocation does

not completely satisfy the boundary conditions. In order to completely satisfy the boundary conditions, an additional stress term must be added to the Airy stress function [3]. It has also been proved [7] that the image dislocation method is conceptually incomplete since it is inconsistent with the cutting operation associated with the formation of free surfaces and also because it is misleading in not considering the stress field of the dislocation in vacuum. In analogy with the electrostatic situation, the image charge has indeed a field associated with it in vacuum. Thus, the image dislocation model, although giving the correct elastic field, is physically inconsistent. Furthermore, it will be shown below that the Green's function method and the image dislocation method cannot be used, at least in their present forms, in understanding the effect of surface energy on the surface boundary conditions, whereas the surface dislocation method can be employed.

The surface dislocation model [7] wherein the surface boundary conditions are satisfied by placing surface arrays of dislocations on the surface is more general and applicable in many situations [8, 9], namely those representing the effect of surface energy or in representing the applied stress on a body or in satisfying the surface boundary conditions in an internally stressed solid. In particular, when the finite body contains an edge dislocation, the surface arrays consist of those with Burgers vector perpendicular to the surface and those with Burgers vector parallel to the surface. The surface dislocation model for an edge dislocation in a semi-infinite solid with its Burgers vector perpendicular to the surface is given in Fig. 1. There are two arrays on the surface. The surface dislocation array with Burgers vector perpendicular to the surface is the primary array since it is the important one in satisfying the boundary conditions, i.e. its energy contribution in the relaxation of the surface is the major one. It is also found that the law of conversation of Burgers vectors of the primary surface array plus the Burgers vector of the lattice dislocation is satisfied [7]. The surface array with Burgers vector parallel to the surface, as shown in Fig. 1, is the secondary array since its contribution to the relaxation of the surface is minor and at the most may be 10% of the total energy. Fig. 2 shows the surface dislocation model of an edge dislocation with Burgers vector parallel to the free surface. The surface array with Burgers vector parallel to the free surface is the primary array and that with Burgers vector perpendicular to the surface is the secondary array. This nomenclature follows the same reasoning as that for an edge dislocation with Burgers vector perpendicular to the surface. It has been proven that the above surface dislocation models give the surface boundary conditions as required by linear elasticity. The surface

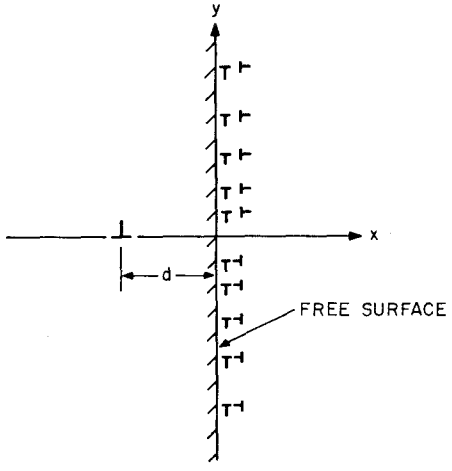

Figure 1 An edge dislocation with Burgers vector perpendicular to the free surface with the surface dislocation arrays consisting of two sets of edge dislocations chosen to satisfy the free surface boundary conditions, $\sigma_{xx} = 0$ and $\sigma_{xy} = 0$ on the $x = 0$ plane.

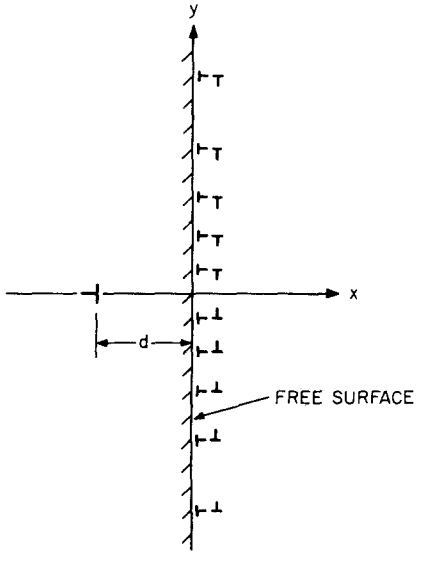

Figure 2 An edge dislocation with Burgers vector parallel to the free surface dislocation arrays consisting of two sets of edge dislocations chosen to satisfy the free surface boundary conditions $\sigma_{xx} = 0$ and $\sigma_{xy} = 0$ on the $x = 0$ plane.

arrays can be obtained by representing them as a continuous distribution of dislocations [10] and their equilibrium distributions can be obtained by making the stress components on them vanish so that they do not move along the surface [7]. Another approach in arriving at the surface distributions, which is more useful in complex geometries of the finite body [8], is the discrete dislocation method. In the discrete dislocation method, the surface array is represented by a set of discrete dislocations and their equilibrium positions can be obtained by minimizing the energy of the configuration [11]. The surface dislocation model is conceptually self-consistent and does not neglect the stress field of any of the dislocations in a vacuum. Thus, the elastic field of the dislocation is obtained after including the stress field of all the dislocations in the surface arrays, and as a natural consequence of screening of the stress field of the lattice dislocation by the surface array, the free surface boundary conditions are satisfied. The relaxation of the surface due to the presence of the surface array is easily understood from Fig. 3.

The surface dislocation array, as shown in Fig. 3, forms steps on the surface which are essential to the relaxation of the surface [12]. These steps consist of dislocation dipoles [13]. In these dipoles, the edge dislocations, shown with full lines, are responsible for the stress field which screens the stress field of the lattice dislocation. The edge dislocations of opposite sign, shown dotted, do not contribute to the stress field but only represent the ledge surface. Since, for every edge dislocation shown with a full line, there is one of opposite sign, the total ledge surface is equal to the total Burgers vector of the surface array. When the boundary conditions of linear elasticity are applied, the stresses on the surface should vanish leading to the conservation of the Burgers vector of the dislocation [7]. Thus, the total ledge surface is equal to the Burgers vector of the primary array, i.e. the Burgers vector of the lattice dislocation. The secondary array also contributes to the ledge area. Although the total Burgers vector of the secondary array, i.e. the algebraic sum of the Burgers vectors is zero, the ledge surface is not zero. When the surface is stress free, the sum of the Burgers vectors of the secondary array on one side of the half space is equal to b_m/π where b_m is the Burgers vector of the lattice dislocation [7].

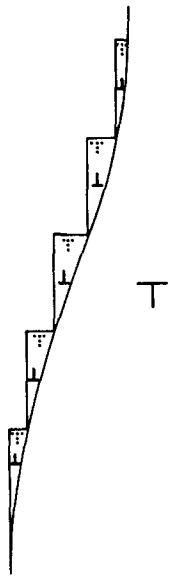

Figure 3 The relaxation of the surface of a semi-infinite body containing a dislocation with Burgers vector perpendicular to the surface. The formation of steps represents the relaxed configuration. Each step consists of dipoles of dislocations. The edge dislocation shown with a full line in each step is responsible for the elastic field and that shown with dotted lines represents the ledge.

The boundary conditions imposed by linear elasticity do not take into account the additional surface area produced by the ledges or steps, i.e. the surface energy contribution to the total energy is assumed to be equal to zero. However, as can be seen from Fig. 3, the ledge surface is an additional surface and if the surface energy is also considered in the total energy, the configuration tends to minimize the surface area. In the process of minimization of surface energy, the surface energy tends to reduce the Burgers vectors of the surface array and also the surface array tends to come closer to the lattice dislocation. Since the surface array is now altered from the original distribution, the surfaces can no longer be stress free. Thus, the effect of surface tension in reducing the surface area of the ledges is to lower the sum of the Burgers vectors of the surface array and also to alter the stress-free surface boundary conditions. In the analysis that follows, the framework of linear elasticity is used to determine the effect of surface energy on the surface dislocation distribution. It should be pointed out that while the magnitude of non-linear effects may be of the same order as the effect of surface energy on the distribution of surface dislocation, the linear

elasticity calculation illustrates the use of surface dislocations in dealing with surface phenomena.

2. Surface dislocation model and the effect of surface energy

It has become clear from the previous illustration that the effect of surface energy is to reduce the overall Burgers vector of the primary and secondary surface arrays. The reduction in the sum of the Burgers vectors also means that the surface arrays will not be present on the surface every where, but will be confined to a region where the interaction between the lattice dislocation and the surface array is a maximum. Fig. 4a shows the surface dislocation model of a lattice dislocation in a semi-infinite solid with its Burgers vector perpendicular to the surface. The interaction between the lattice dislocation and the surface array decreases as the distance from the dislocation in the y-direction increases. Therefore, the surface array will be confined to a region $-L < y < L$. In the region outside $|y| > L$. the stress field due to the dislocation is not sufficient to generate a surface ledge because the increase in surface energy is not balanced by the reduction in energy due to relaxation of the surface by formation of the ledge. The surface energy tends to reduce the surface area while the stress due to the dislocation forces the surface to relax and thus form the surface array and the associated ledge steps. Fig. 4b shows the surface dislocation model with the secondary array only. While the primary array responds to σ_{xx} component of stress of the lattice dislocation, the secondary array does so with respect to the σ_{xy} component. Since the σ_{xy} component of the stress field interacts to the maximum extent at $|y| = d$ with the secondary array and since the interaction is zero at $y = 0$, the surface array tends to become concentrated at $y = \pm d$. The surface energy tends to reduce the total Burgers vector of the surface array but the stress field, due to the dislocation, forces the surface to relax. The result is the distribution of dislocations in the region $L_1 < |y| < L_2$ with a maximum near $|y| = d$. The dislocation distribution in the secondary array is obtained by equating the σ_{xy} component on each dislocation to zero.

Fig. 5a gives the surface dislocation model when the Burgers vector of the lattice dislocation is parallel to the free surface. The

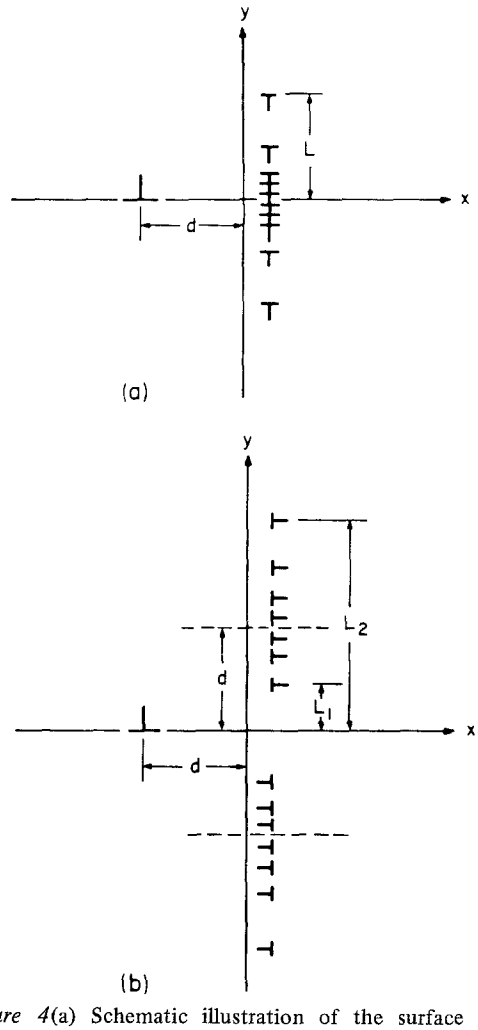

Figure 4(a) Schematic illustration of the surface dislocations in the primary surface array on the surface of a semi-infinite solid containing an edge dislocation with Burgers vector perpendicular to the free surface. Note that the configuration is symmetrical about the x-axis. (b) Schematic illustration of the surface dislocations in the secondary surface array on the surface of a semi-infinite solid containing an edge dislocation with Burgers vector perpendicular to the free surface. Note that the configuration is asymmetric about the x-axis.

primary array consists of dislocations with Burgers vector parallel to the free surface. The interaction between the σ_{xy} component of stress of the lattice dislocation and the primary array is not a maximum at the centre. Therefore, when the surface is stress-free, i.e. $\gamma = 0$, the distribution becomes zero at $y = 0$. The effect of surface energy is to push the point of zero stress to either side on the y-axis. Thus the primary array will be spread in the region $L_1 < |y| < L_2$. Outside this region, the σ_{xy} component of stress is not sufficient to create a surface ledge

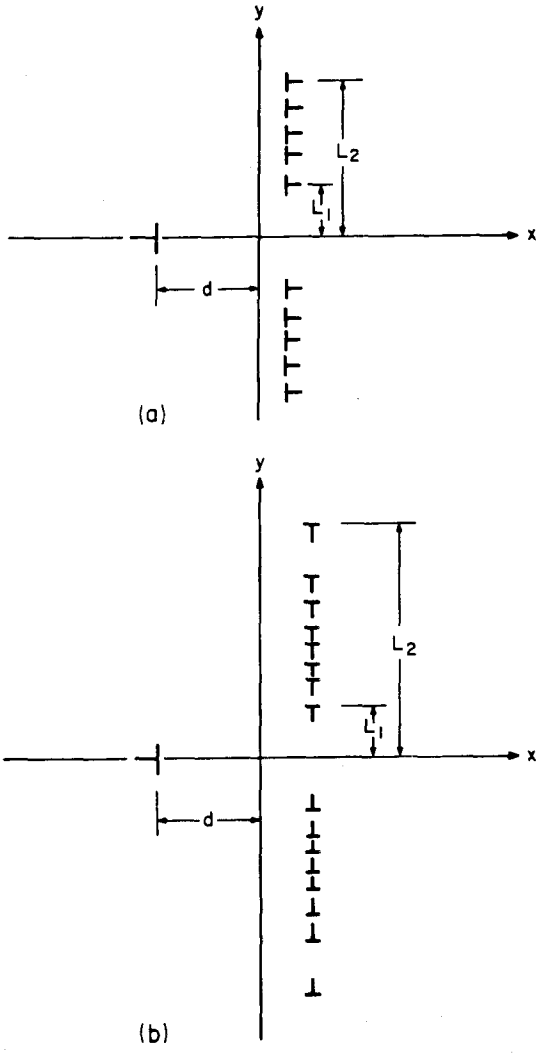

Figure 5(a) Same as Fig. 4a except that the lattice dislocation is parallel to the free surface and the primary surface array also has a parallel Burgers vector. Note that the array lies in the region $L_1 < |y| < L_2$. (b) Same as Fig. 4b except that the lattice dislocation is parallel to the free surface and the secondary surface array has a Burgers vector perpendicular to the surface.

since the surface energy of the ledge dominates. The dislocation distribution is an even function of y and bounded at both the end points and throughout the region of its definition.

Fig. 5b shows the surface dislocation model of the secondary array only which relaxes the σ_{xx} component of stress. Since the σ_{xx} component of stress has the maximum interaction with the surface array at $|y| = d$, the distribution reaches a maximum near $|y| = d$. Also, the interaction is zero at $y = 0$ and hence the effect of surface energy is to spread the surface array in the region $L_1 < |y| < L_2$. The equilibrium distribution of the secondary array can be obtained by making the σ_{xx} component of stress vanish. The distribution of the secondary array of dislocations is an odd function of y and it is bounded at the end points and in the region of its definition.

In order that both the stress components due to the lattice dislocation are relaxed to the extent that the configuration allows it, both the surface arrays, i.e. the primary and the secondary should be superimposed. Thus, Figs. 4 and 5 constitute the surface dislocation model of an edge dislocation in a semi-infinite solid with the effect of surface energy considered. It is now clear from the present analysis that the stresses do not vanish on the surface for any solid containing an internal source of stress, if the effect of surface energy is considered.

3. Analysis of surface dislocation distributions

In the following, the dislocation distributions associated with surface array illustrated in Figs. 4 and 5 will be obtained using the method of continuously distributed dislocations [10]. The equilibrium in the primary array in Fig. 4a is given by allowing the σ_{xx} component on each dislocation to become zero, thus

$$\int_{-L}^{L} \frac{f_1(y_i)\mathrm{d}y_i}{y - y_i} = \frac{b_m}{b_i}\left[\frac{3y}{y^2 + d^2} - \frac{2y^3}{(y^2 + d^2)^2}\right], \tag{1}$$

where b_m is the Burgers vector of the lattice dislocation, b_i is the Burgers vector of each dislocation in the surface array, while $f_1(y_i)$ is the dislocation distribution of the surface array in the region $-L < y < L$ which should be determined from the above equation. The above integral equation can be inverted to obtain a bounded distribution function by imposing the condition that $f_1(y)$ should be an even function of y [14]. The result is

$$f_1(y) = \frac{2b_m}{\pi b_i}(L^2 - y^2)^{1/2}\left[\frac{d^2}{2(L^2 + d^2)^{1/2}(y^2 + d^2)} + \frac{d^3}{(d^2 + L^2)^{1/2}(y^2 + d^2)^2} - \frac{L^2 d}{2(L^2 + d^2)^{3/2}(y^2 + d^2)}\right]. \tag{2}$$

It is seen from Equation 2 that the function is even and also bounded at the end points and everywhere in the region of its definition. Equation 2 by itself is not completely defined since the value of L is not fixed. The value of L is fixed by imposing the condition that the energy of the configuration should be a minimum. Since the self energy of the lattice dislocation is constant, the energy of the configuration which should be minimized is given by

$$E_T = \frac{G\boldsymbol{b}_i^2}{2\pi(1-\nu)} \log\left(\frac{4R}{\boldsymbol{b}_i}\right) \int_0^L f_1(y)\mathrm{d}y + 2\gamma \boldsymbol{b}_i \int_0^L f_1(y)\mathrm{d}y - \frac{G\boldsymbol{b}_i\boldsymbol{b}_m}{\pi(1-\nu)} \int_0^L \left[\log\left(\frac{R}{R_{12}}\right) - \frac{y^2}{d^2+y^2}\right] \cdot f_1(y)\mathrm{d}y + \frac{G\boldsymbol{b}_i^2}{\pi(1-\nu)} \int_0^L \int_y^L \left[\log\left(\frac{R}{R_{13}}\right) - 1\right] f_1(y) f_1(t)\mathrm{d}y\mathrm{d}t + \frac{G\boldsymbol{b}_i^2}{2\pi(1-\nu)} \int_0^L f_1(y)\mathrm{d}y \int_0^L \left[\log\left(\frac{R}{R_{14}}\right) - 1\right] f_1(t)\mathrm{d}t, \quad (3)$$

where $R_{12} = (d^2 + y^2)^{1/2}$, $R_{13} = t - y$ and $R_{14} = t + y$. R in the above equation is the size of the crystal which, for computational purposes, was chosen to be very large, i.e. $R = 1$ cm. The shear modulus, G and Poisson's ratio, ν were chosen to be those of iron and γ, the surface energy, is 2000 ergs cm^{-2} for iron [3]. In the above equation, the first term represents the self energy of the array of surface dislocations, the second term, the surface energy due to the formation of the ledges, the third term, the interaction between the lattice dislocation and the surface array and the fourth and fifth terms, the interaction energy of the array of surface dislocations among themselves. The function $f_1(y)$ can be substituted from Equation 2 and E_T evaluated. But since the integrals are cumbersome to evaluate, numerical computational procedures have been adopted [11] to minimize the value of E_T with respect to $\boldsymbol{b}_i$ and L. In particular, the integrals have been evaluated using QG10, the built-in scientific subroutine package of IBM, which uses the 10 point Gaussian quadrature formula. The value of L in Å where E_T reached its minimum value for a given value of γ is shown in Fig. 6 for the position of the dislocation, $d = 10$ Å. Although the value of γ for any medium is fixed, it is used here as a parameter to study the effect of surface energy. It is seen from Fig. 6 that L decreases very fast initially with increasing γ but only gradually with increasing γ at higher values of γ. The total Burgers vector associated with the surface array is obtained from

$$b_T = 2b_i \int_0^L f_1(y)\mathrm{d}y, \quad (4)$$

and is shown in Fig. 7 as a function of γ. It is seen that with decreasing γ, $\boldsymbol{b}_T$ approaches $\boldsymbol{b}_m$ indicating that the law of conservation of Burgers vectors is satisfied only for $\gamma = 0$. The decrease in the value of $\boldsymbol{b}_T$ with γ is very small initially but large for higher values of γ. The energy of the configuration, excluding the self energy of the lattice dislocation, given by Equation 3, is shown in Fig. 8 as a function of γ. It is seen that the total energy, E_T increases with increasing γ. The

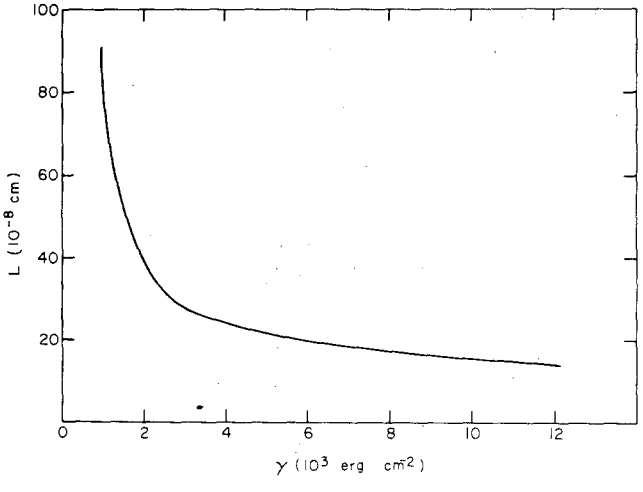

Figure 6 The length to which the primary surface array is spread over the surface of a semi-infinite solid obtained by minimization of Equation 3 shown as a function γ for $d = 10$ Å.

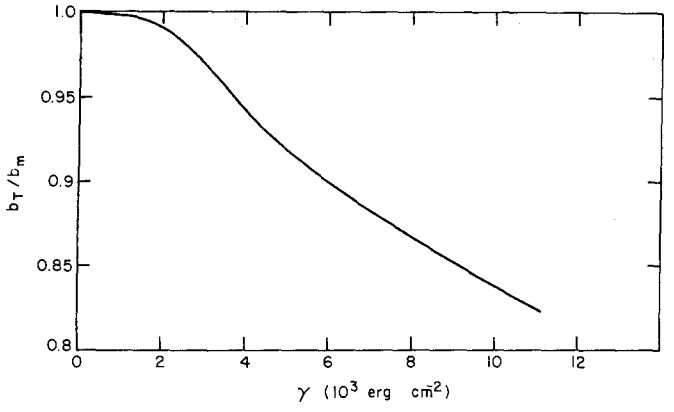

Figure 7 The total Burgers vector $\boldsymbol{b}_T$ contained in the primary surface array given by Equation 4 shown as a function of γ for $d = 10$ Å.

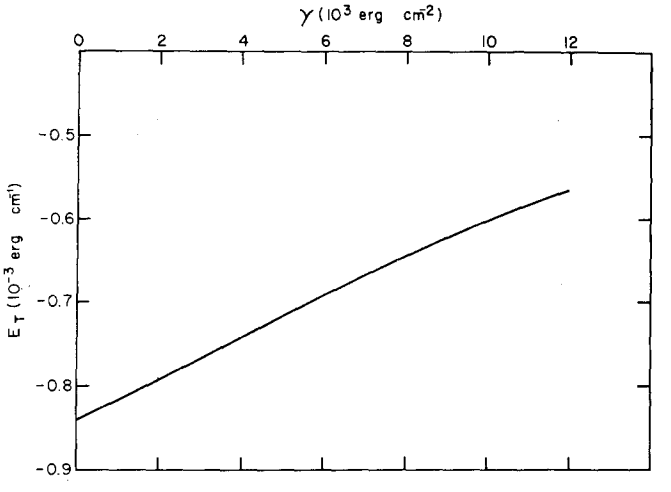

Figure 8 E_T given by Equation 3, when minimized, shown as a function of γ for $d = 10$ Å.

distribution function $f_1(y)$ given by Equation 2 is shown in Fig. 9 for various values of γ. It shall be noted that although the distribution function is greatest at the same value of y/L, this has no significance since it is the value of L which determines the total Burgers vector within the surface array. However, it is seen that with increasing γ, the distribution function decreases more gradually. It should also be noted that when $\gamma = 0$, the value of L goes to infinity and the distribution function becomes that with free surface boundary conditions.

The dislocation distribution associated with the secondary array of dislocations shown in Fig. 4b can be obtained by allowing the σ_{xy} component of stress on each dislocation to vanish. The equilibrium of the surface array is given by

$$\int_{-L_2}^{-L_1} \frac{f_2(y_i)\,dy_i}{y - y_i} + \int_{L_1}^{L_2} \frac{f_2(y_i)\,dy_i}{y - y_i} = \frac{\boldsymbol{b}_m\, d(y^2 - d_i^2)}{\boldsymbol{b}_i (y^2 + d^2)^2} \qquad (5)$$

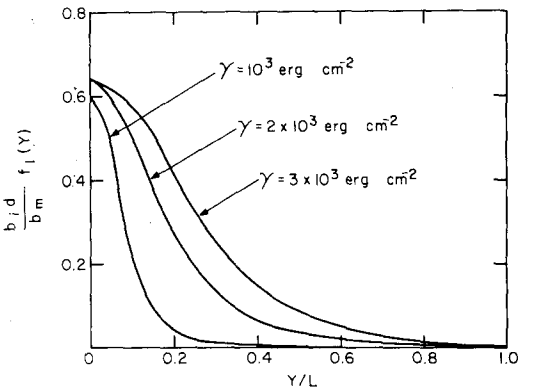

Figure 9 The distribution function $f_1(y)$ shown in a dimensionless form as a function of y/L for three values of γ and $d = 10$ Å.

Since the distribution function is odd and it is bounded at the end points, it can be inverted in the usual manner. The result is

$$f_2(y) = \pm \frac{\boldsymbol{b}_m d}{\pi b_i} \frac{[(y^2 - L_1^2)(L_2^2 - y^2)]^{1/2}}{[(L_1^2 + d^2)(L_2^2 + d^2)]^{1/2}}$$

$$\times\left[\frac{d^2}{(d^2+y^2)(L_1^2+d^2)}\right.$$

$$\left.+\frac{d^2}{(d^2+y^2)(L_2^2+d^2)}-\frac{(y^2-d^2)}{(y^2+d^2)^2}\right] \quad (6)$$

with $L_2L_1 = d^2$ and the plus sign is used in the positive half plane and the negative sign in the negative half plane. It is seen that the distribution function is bounded at the end points and everywhere else, in the region of its definition. It is also seen that when $L_1 = 0$ and $L_2 \to \infty$, the distribution function reduces to that in a semi-infinite medium with free surface boundary conditions. Equation 6 by itself is not completely defined since the values of L_1 and L_2 are not fixed. The values of L_1 and L_2 are determined by imposing the condition that the energy of the configuration should be a minimum. Since the self energy of the lattice dislocation is constant, the energy of the configuration which should be minimized is given by

$$E_T = \frac{Gb_i^2}{2\pi(1-\nu)}\log(4R/b_i)\int_{L_1}^{L_2} f_2(y)\mathrm{d}y$$

$$+ 2\gamma b_i\int_{L_1}^{L_2} f_2(y)\mathrm{d}y - \frac{Gb_ib_m d}{\pi(1-\nu)}\int_{L_1}^{L_2}\frac{yf_2(y)\mathrm{d}y}{d^2+y^2}$$

$$+\frac{Gb_i^2}{\pi(1-\nu)}\int_{L_1}^{L_2}\int_{y}^{L_2}\log\left(\frac{R}{R_{13}}\right)f_2(y)f_2(t)\mathrm{d}t\mathrm{d}y$$

$$-\frac{Gb_i^2}{2\pi(1-\nu)}\int_{L_1}^{L_2} f_2(y)\mathrm{d}y\int_{L_2}^{L_2}\log\left(\frac{R}{R_{14}}\right)f_2(t)\mathrm{d}t \quad (7)$$

where $R_{13} = t - y$ and $R_{14} = t + y$. The terms in the order shown have the same significance as those in Equation 3. Equation 7 has been minimized numerically as described earlier [11] to determine L_1 and L_2 as a function of γ. The integrals are evaluated using the built-in subroutine QG10. The values of L_1 and L_2 where E_T given by Equation 7 reaches a minimum value are shown in Fig. 10 as a function of γ for the position of the dislocation, $d = 10$ Å. Although

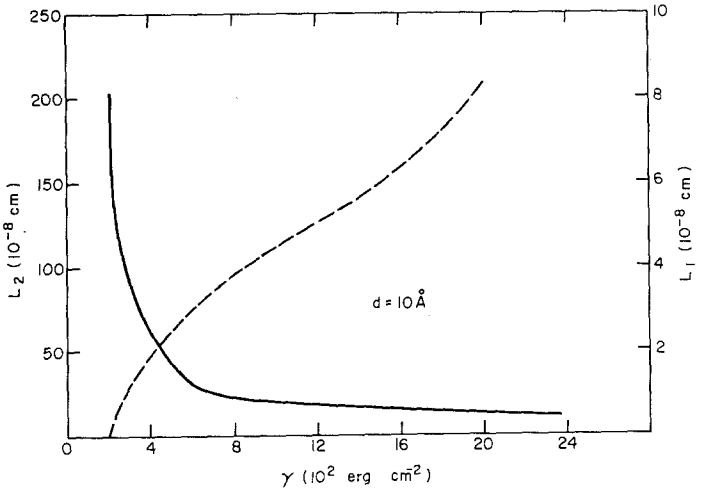

Figure 10 The upper limit L_2 and the lower limit L_1 along the y-axis in which the secondary surface array is distributed, obtained after minimizing Equation 7 and shown as a function of γ for $d = 10$ Å. The dotted line corresponds to L_1 and the full line to L_2.

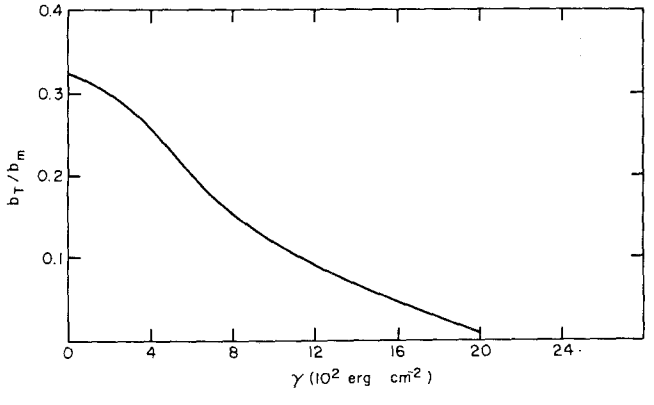

Figure 11 The total Burgers vector of the secondary surface array defined by Equation 8 shown as a function of γ for $d = 10$ Å.

the value of γ for any medium is fixed, it is used here as a parameter in order to study the effect of surface energy. It is seen from Fig. 10 that L_2 decreases very fast initially with increasing γ but only slowly at higher values of γ. The lower limit L_1 increases almost gradually with increasing γ for all values of γ. It is seen that with increasing γ, the upper limit L_2 and the lower limit L_1 approach the value of d indicating that the length of the distribution of the surface array decreases. Since the stress field σ_{xy} of the lattice dislocation is a maximum at $|y| = d$, both the limits approach d, thus decreasing the total Burgers vector associated with surface array with increasing γ. The total Burgers vector within the surface array on one side of the y-axis is given by

$$\boldsymbol{b}_T = \boldsymbol{b}_i \int_{L_1}^{L_2} f_2(y)\mathrm{d}y, \qquad (8)$$

and is shown in Fig. 11 as a function of γ. $\boldsymbol{b}_T$ approaches $\boldsymbol{b}_m/\pi$ indicating that the principle of minimum energy leads to that of the free surface boundary conditions [7] when $\gamma = 0$. The decrease in the value of $\boldsymbol{b}_T$ with increasing γ is gradual. However, it is important to note that when γ reaches 2×10^3 erg cm^{-2}, the secondary surface array under the distribution function completely vanishes, indicating that the effect of surface energy on the secondary surface array is very large. This result for iron also indicates that the σ_{xy} component due to a lattice dislocation does not vanish on the surface since for $\gamma \sim 2000$ ergs cm^{-2}, the secondary surface array almost completely vanishes. It is seen from Fig. 12 that the total energy E_T increases with γ and becomes positive if γ exceeds 2×10^3 ergs cm^{-2}, which indicates that the surface energy of the ledge is more than the energy of relaxation produced due to its formation. The distribution function $f_2(y)$ given by Equation 6 is shown in Fig. 13 for various values of γ. The co-ordinate takes zero value at L_1 and reaches unity at L_2. It is seen that the distribution function reaches a maximum at some value of y between L_1 and L_2 and this position of the maximum shifts as γ increases. The above analysis completes the surface dislocation model for an edge dislocation with Burgers vector perpendicular to the surface.

The analysis of the surface dislocation model for an edge dislocation with Burgers vector parallel to the surface is given by analysing the primary and secondary surface arrays in Fig. 5a and b. The dislocation distribution function representing the primary surface array in Fig. 5a is obtained by making the σ_{xy} component of stress vanish on each dislocation in the array. The corresponding equilibrium condition is given by

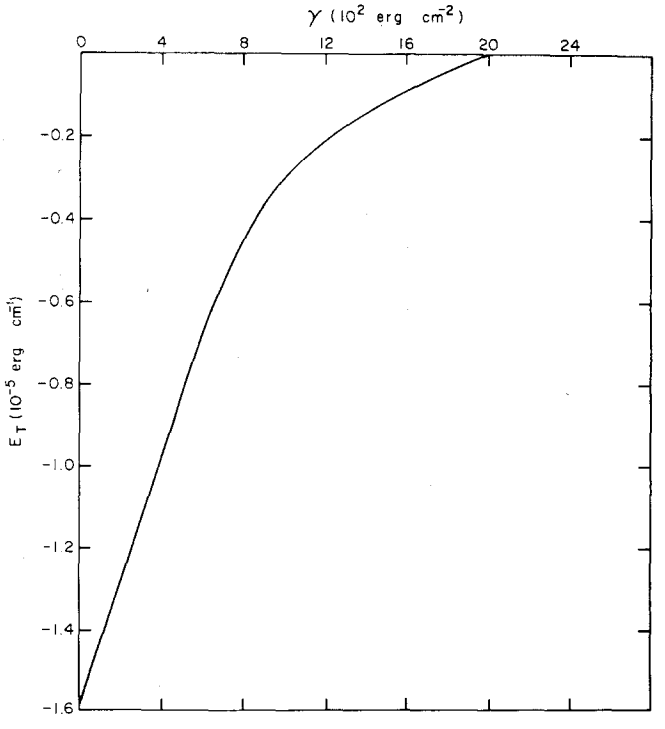

Figure 12 The energy of the configuration of the secondary array when minimized, given by Equation 7, shown as a function of γ for $d = 10$ Å.

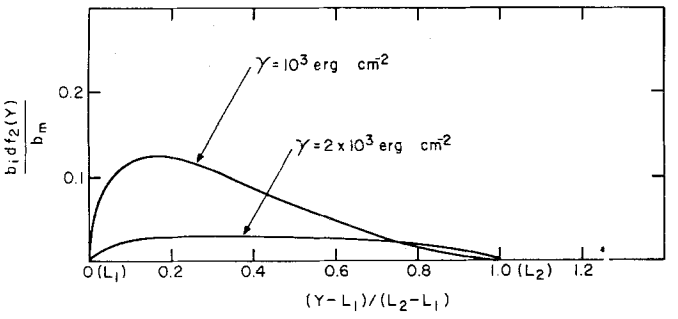

Figure 13 The distribution function $f_2(y)$ shown in a dimensionless form as a function of $(y - L_1)/(L_2 - L_1)$ for two values of γ and for $d = 10$ Å. Note that the maximum in the distribution function shifts with increasing γ.

$$\int_{-L_2}^{-L_1} \frac{f_3(y_i)\mathrm{d}y}{y - y_i} + \int_{L_1}^{L_2} \frac{f_3(y_i)\mathrm{d}y_i}{y - y_i} = \frac{\boldsymbol{b}_m y(d^2 - y^2)}{\boldsymbol{b}_i(y^2 + d^2)^2}. \quad (9)$$

Since the distribution function $f_3(y_i)$ is even and bounded at the end points and everywhere in the region of its definition, it can be evaluated to be

$$f_3(y) = \frac{\boldsymbol{b}_m y[(y^2 - L_1^2)(L_2^2 - y^2)]^{1/2}}{\pi \boldsymbol{b}_i[(L_1^2 + d^2)(L_2^2 + d^2)]^{1/2}} \left[\frac{d^2}{(d^2 + y^2)(L_1^2 + d^2)} + \frac{d^2}{(d^2 + y^2)(L_2 + d^2)} - \frac{(y^2 - d^2)}{(y^2 + d^2)^2} \right] \quad (10)$$

with $L_2 L_1 = d^2$. The terms $\boldsymbol{b}_m$ and $\boldsymbol{b}_i$ have the same meaning as earlier. The distribution function given by Equation 10 is bounded at the end points and becomes that for a semi-infinite medium with a free surface when $L_2 \to \infty$ and $L_1 \to 0$.

The quantities L_1 and L_2 in Equation 10 are fixed by superimposing the condition that the energy of the configuration should be minimum. Since the self energy of the lattice dislocation is constant, the energy of the configuration which should be minimized is given by

$$E_T = \frac{G\boldsymbol{b}_i^2}{2\pi(1-\nu)} \log\left(\frac{4R}{\boldsymbol{b}_i}\right) \int_{L_1}^{L_2} f_3(y)\mathrm{d}y + 2\gamma \boldsymbol{b}_i \int_{L_1}^{L_2} f_3(y)\mathrm{d}y - \frac{G\boldsymbol{b}_i\boldsymbol{b}_m}{\pi(1-\nu)} \times \int_{L_1}^{L_2} \left[\log\left(\frac{R}{R_{12}}\right) - \frac{d^2}{d^2 + y^2} \right] \cdot f_3(y)\mathrm{d}y + \frac{G\boldsymbol{b}_i^2}{\pi(1-\nu)} \int_{L_1}^{L_2} \int_{y}^{L_2} \log\left(\frac{R}{R_{13}}\right) f_3(y) f_3(t)\mathrm{d}y\mathrm{d}t + \frac{G\boldsymbol{b}_i^2}{2\pi(1-\nu)} \int_{L_1}^{L_2} f_3(y)\mathrm{d}y \cdot \int_{L_1}^{L_2} \log\left(\frac{R}{R_{14}}\right) f_3(t)\mathrm{d}t, \quad (11)$$

where $R_{12} = (d^2 + y^2)^{1/2}$, $R_{13} = t - y$ and $R_{14} = t + y$. All the terms in the above equation

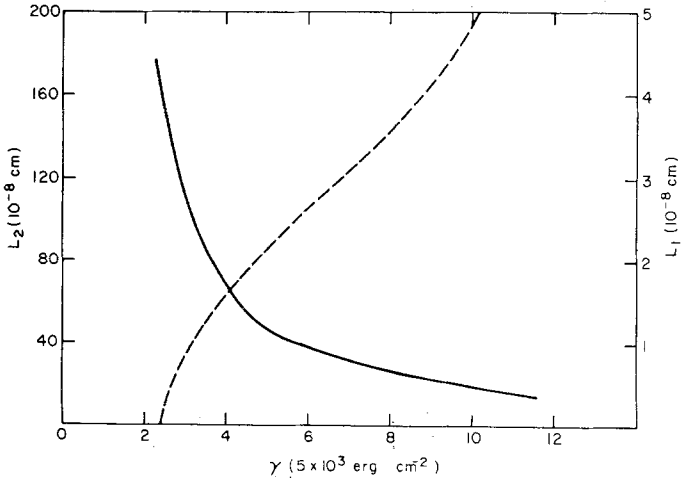

Figure 14 Values of L_1 and L_2 obtained by minimizing E_T, given by Equation 11 shows as a function of γ for $d = 10$ Å. The full line corresponds to L_2 and the dotted line to L_1.

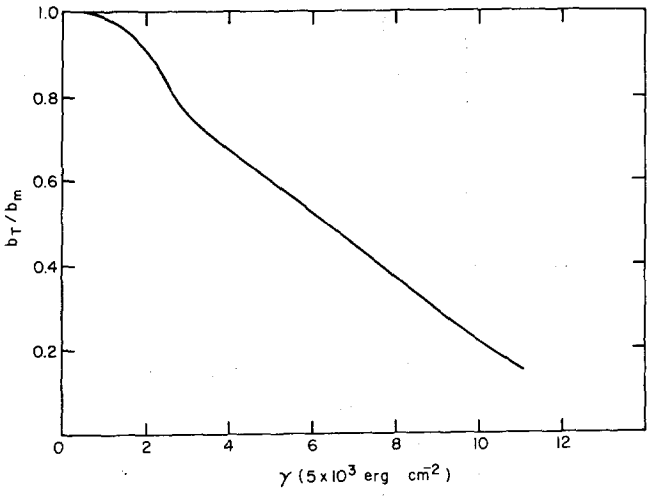

Figure 15 The total Burgers vector, b_T, contained in the primary surface array defined by Equation 12 and shown as a function of γ for $d = 10$ Å.

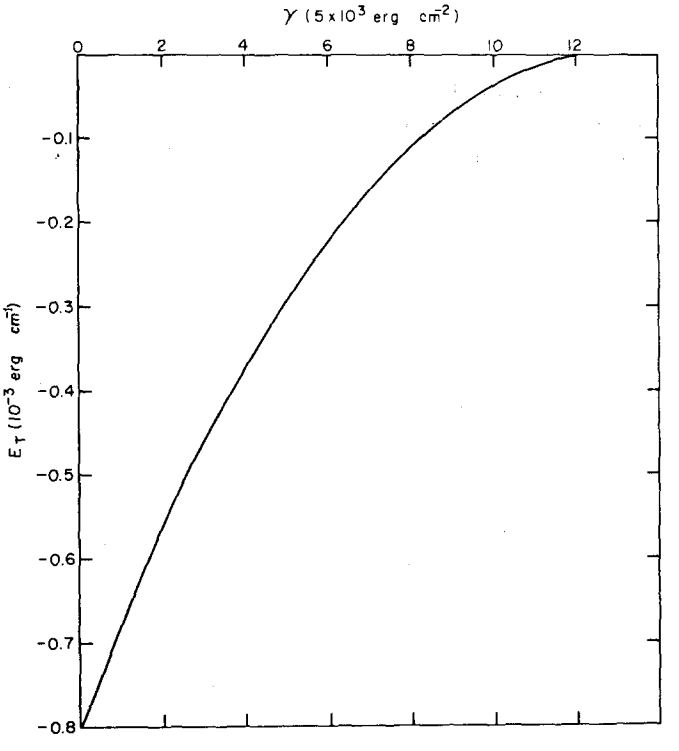

Figure 16 E_T, the total energy of the configuration when minimized, given by Equation 11 shown as a function of γ for $d = 10$ Å.

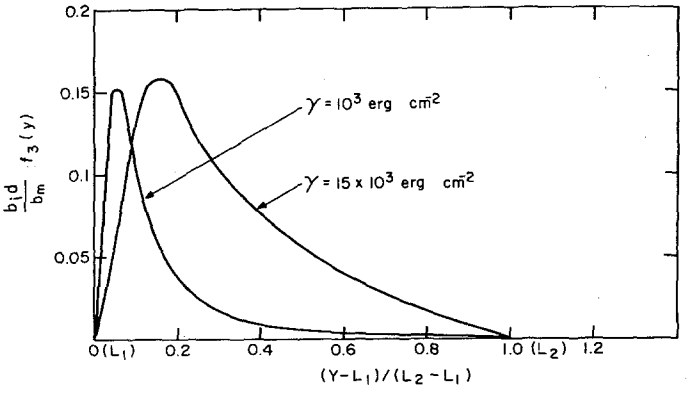

Figure 17 The distribution function $f_3(y)$ in the dimensionless form given by Equation 10 and shown as a function of $(y - L_1)/(L_2 - L_1)$ for two values of γ for $d = 10$ Å.

have the same significance in the order shown as those in Equation 3. E_T has been minimized as a function of γ to arrive at value of L_1 and L_2 and the computational procedures used are the same as those given earlier. The values of L_1 and L_2 obtained from the minimization procedure are shown in Fig. 14 as a function of γ. Although the value of γ is fixed for any medium, the effect of surface energy becomes evident from Fig. 14. It is seen that L_2 decreases very fast initially but only gradually at higher values of γ. The quantity L_1 increases gradually at all γ. It is seen that the lower limit is increased nearly 5 Å above the $y = 0$ axis if γ is increased to a very large value. At $\gamma = 2000$, which is the value for iron, it is seen that L_1 is equal to zero. It is also seen from Fig. 14 that the effect of surface energy on the primary surface array is much smaller compared to the effect on the primary surface array for an edge dislocation whose Burgers vector is perpendicular to the surface. This may be due to the fact that the surface array, when the Burgers vector is parallel to the surface, is spread to very large distances from the dislocation. The total Burgers vector, $\boldsymbol{b}_T$ contained in surface array is defined as

$$\boldsymbol{b}_T = 2\boldsymbol{b}_i \int_{L_1}^{L_2} f_3(y)\mathrm{d}y \qquad (12)$$

and is shown as a function of γ in Fig. 15. It is seen that $\boldsymbol{b}_T$ decreases very rapidly initially but only gradually at higher values of γ, as γ increases. The total energy of the configuration E_T given by Equation 11 is shown in Fig. 16 as a function of γ. It is seen that in order to eliminate the surface array completely, a very high value of the surface energy is required. The distribution function $f_3(y)$ given by Equation 10 is shown for two values of γ in Fig. 17. The co-ordinate axis becomes zero at $y = L_1$ and unity at $y = L_2$. It is seen that the maximum in the distribution function shifts away from the $y = 0$ line as γ increases. It is also to be noted that even when $y = 0$, the maximum in the distribution is not at the origin for the reason mentioned earlier.

The dislocation distribution associated with the secondary array of dislocations shown in Fig. 5b can be obtained by making the σ_{xx} component of stress on each dislocation vanish. The equilibrium of the surface array is given by Equation 5 and the distribution function is given by Equation 6. However, the values of L_1 and L_2 are obtained by imposing the condition that the energy of the configuration should be a minimum. Since the self energy of the lattice dislocation is constant, the energy of the configuration which should be minimized is given by

$$\begin{aligned} E_T = {} & \frac{Gb_i^2}{2\pi(1-\nu)} \log\left(\frac{4R}{b_i}\right) \int_{L_1}^{L_2} f_2(y)\mathrm{d}y \\ & + 2b_i\gamma \int_{L_1} f_2(y)\mathrm{d}y \\ & - \frac{Gb_ib_m d}{\pi(1-\nu)} \int_{L_1}^{L_2} \frac{yf_2(y)\mathrm{d}y}{d^2+y^2} \\ & + \frac{Gb_i^2}{\pi(1-\nu)} \int_{L_1}^{L_2} \int_{y}^{L_2} \left[\log\left(\frac{R}{R_{13}}\right) - 1\right] f_2(y)f_2(t)\mathrm{d}t\mathrm{d}y \\ & - \frac{Gb_i^2}{2\pi(1-\nu)} \int_{L_1}^{L_2} f_2(y)\mathrm{d}y \cdot \\ & \int_{L_1}^{L_2} \left[\log\left(\frac{R}{R_{14}}\right) - 1\right] f_2(t)\mathrm{d}t \end{aligned} \qquad (13)$$

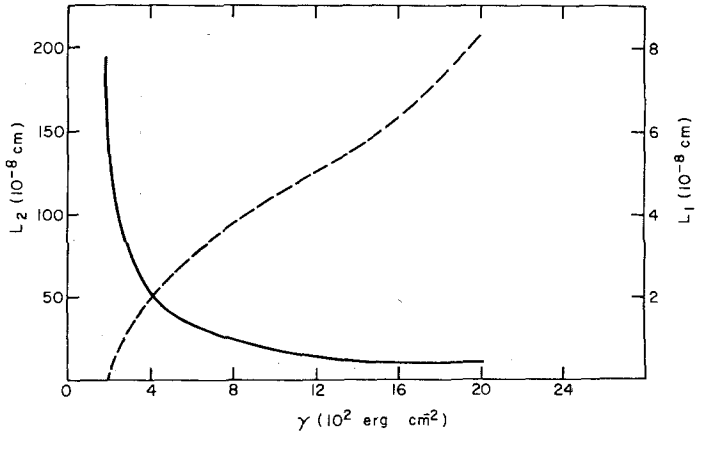

Figure 18 L_1 and L_2 obtained as a result of minimization of E_T given by Equation 13 shown as a function of γ for $d = 10$ Å. The full line indicates the values of L_2 and the dotted line that of L_1.

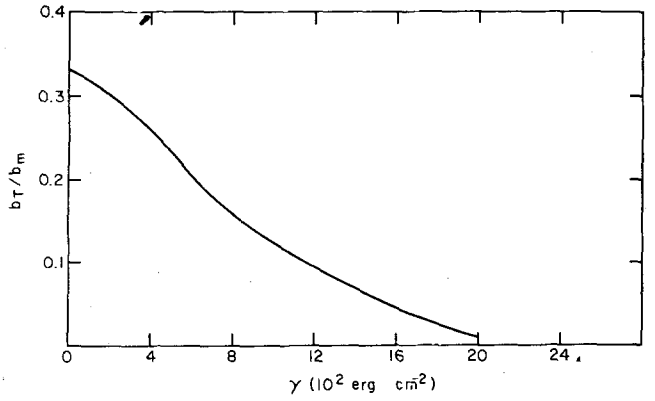

Figure 19 b_T, the total Burgers vector contained in the secondary surface array near a lattice dislocation with Burgers vector parallel to the surface shown as a function of γ for $d = 10$ Å. The definition of b_T is given by Equation 8.

where $R_{13} = t - y$ and $R_{14} = t + y$. The terms in the order shown have the same significance as those in Equation 7. Equation 13 has been minimized in order to determine the values of L_1 and L_2 as a function of γ. Comparison of Fig. 18, where L_1 and L_2 are shown as a function of γ, with Fig. 10 shows that the variation of L_1 and L_2 is almost the same. Similarly, b_T, the total Burgers vector under the surface array defined by Equation 8 and shown in Fig. 19 has the same relationship to γ as shown earlier in Fig. 11. Thus, the secondary surface array, although of different orientation when the lattice dislocation is perpendicular or parallel to the interface, bears the same relationship to γ. The total energy E_T obtained at different values of γ is shown in Fig. 20 and it has the same dependence on γ as was seen in Fig. 12. Thus, the secondary surface arrays need not be considered separately for the two orientations of dislocations, even when the effect of surface energy is taken into account. It should also be noted that the secondary surface array vanishes completely when the surface energy reaches a value of 2000 erg cm^{-2}.

4. Discrete dislocation analysis

The previous results have been obtained using the method of continuously distributed dislocations. As mentioned earlier, the analysis of the surface dislocation array can also be made using the

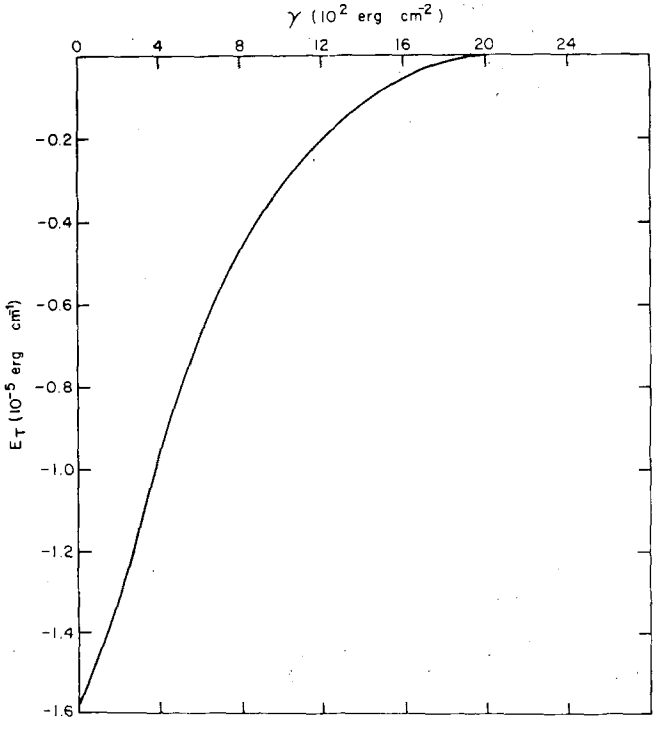

Figure 20 E_T, the total energy of the configuration when minimized, given by Equation 13 shown as a function of γ for $d = 10$ Å.

discrete dislocation method. The discrete dislocation method uses the same principles employed earlier except that the surface array is now represented by discrete dislocations. In the discrete dislocation method, the total energy of the configuration is minimized with respect to the positions of the dislocation array. In particular, when the primary surface array in Fig. 4a is determined, the total energy of the configuration is given by

$$E_T = 2N_s \frac{Gb_i^2}{4\pi(1-\nu)} \log\left(\frac{4R}{b_i}\right) + 2N_s\gamma b_i + \sum_{j=i+1}^{N_s}\sum_{i=1}^{N_s} \frac{Gb_i^2}{\pi(1-\nu)}\left[\log\left(\frac{R}{R_{12}}\right) - 1\right] + \sum_{j=1}^{N_s}\sum_{i=1}^{N_s} \frac{Gb_i^2}{2\pi(1-\nu)}\left[\log\left(\frac{R}{R_{13}}\right) - 1\right] - \sum_{i=1}^{N_s} \frac{Gb_i b_m}{\pi(1-\nu)} \times \left[\log\frac{R}{(d^2+y_i^2)^{1/2}} - \frac{y_i^2}{(d^2+y_i^2)}\right], \quad (14)$$

where $R_{12} = y_j - y_i$, $R_{13} = y_j + y_i$ and y_i and y_j are the positions of the ith and jth surface dislocations in the array. In the above equation, the self energy of the lattice dislocation is not considered since it is a constant term. The first term in the above equation is the self energy of all the surface dislocations numbering $2N_s$, the second term their contribution to the surface energy, the third term, the interaction energy of the surface arrays on either side of the y-axis, the fourth term, the interaction energy of the surface array on the positive y-axis with those on the negative y-axis and the fifth term, the interaction energy between the lattice dislocation of Burgers vector, b_m with all the dislocations in the surface array. Equation 14 is minimized with respect to the positions of all the N_s variables, i.e. the positions of dislocations in the surface array. It is also minimized with respect to the number of dislocations, i.e. surface dislocations are added to the surface as long as the energy of the configuration decreases. In the above equation, the effect of surface energy is taken into account through the ledge surface energy. Equation 14 is essentially similar to the earlier equations of energy written in the continuous distribution method; although here the dislocations are discrete, whereas they are distributed continuously in the earlier method. The energy of the configuration is shown in Fig. 21 as a function of γ. The shear

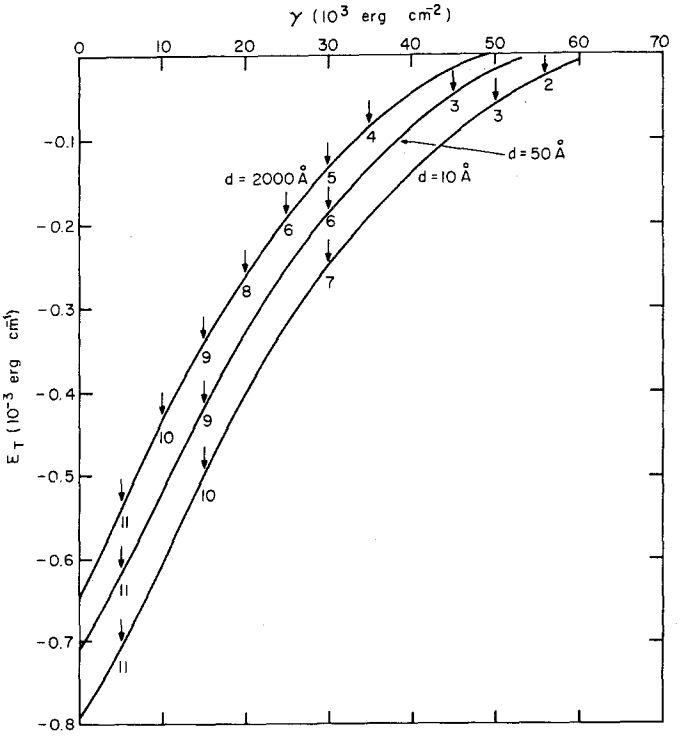

Figure 21 E_T given by Equation 14 obtained from the discrete dislocation method by minimization with respect to the positions of all the dislocations. The arrows indicate the number of surface dislocations present at the value of γ specified on the x-axis, but only on one half of the surface.

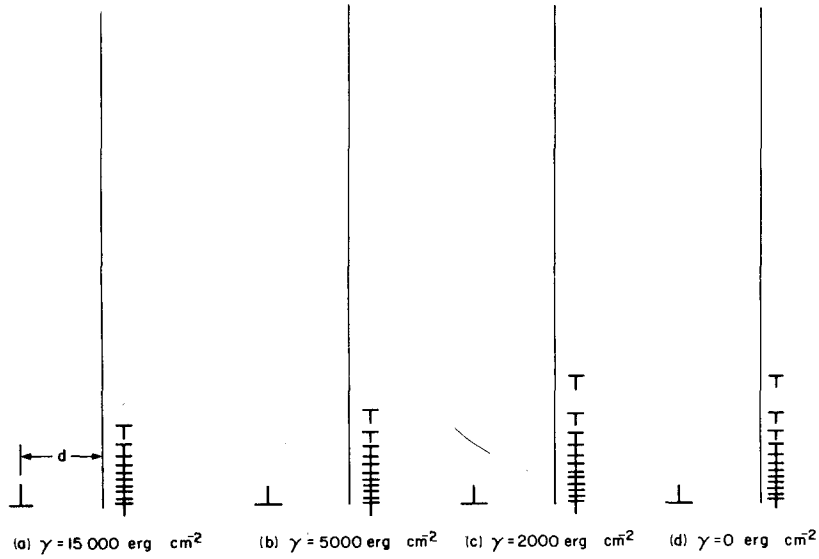

Figure 22 The dislocation configuration of the primary dislocation array on the surface of a semi-infinite solid containing a dislocation with Burgers vector perpendicular to the surface. The lattice dislocation is separated by 10 Å from the surface.

modulus and Poisson's ratio have been assumed to possess the same values mentioned earlier. The lattice dislocation has a Burgers vector, $\boldsymbol{b}_m = 2.4$ Å. The surface dislocations are assumed to possess a Burgers vector of magnitude $\boldsymbol{b}_i = 0.1$ Å. The arrow at each point and the number associated with each arrow indicates the energy of the configuration and the number of surface dislocations N_s in the surface array. It is seen from Fig. 21 that in order to eliminate the surface array completely, a very high value of surface energy is required. The dislocation is separated from the surface by $d = 10$ Å. It is seen that with increasing surface energy, the surface array comes closer to the lattice dislocation because there are a smaller number of lattice dislocations in the array.

The discrete dislocation method can also be carried out using the same principles as that for the secondary surface array. The energy of the configuration will again be given by an equation similar to Equation 14 with the difference that the interaction enegy of the dislocations in the secondary array and the interaction of the lattice dislocations with the secondary array should be replaced by new terms. The energy associated with the configuration of the secondary array of dis-

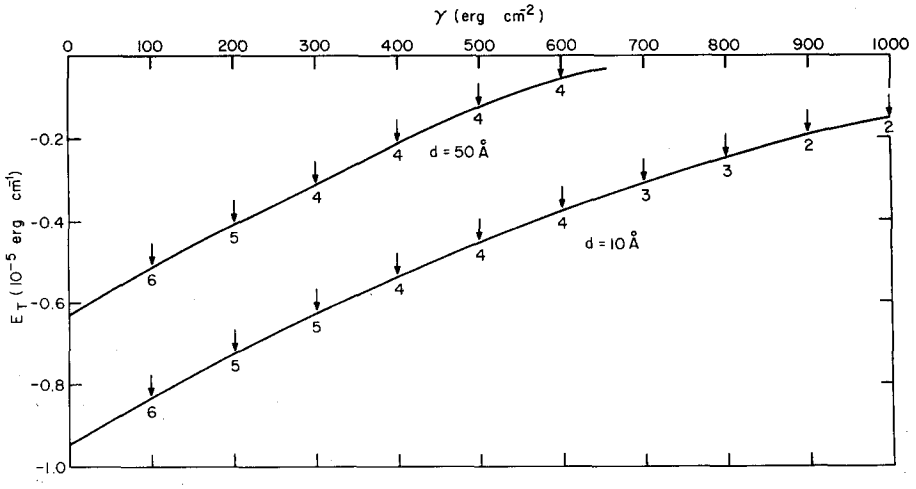

Figure 23 E_T, the total energy of the configuration obtained by the minimization procedure using the discrete dislocation method. The arrows and the associated numbers indicate the number of surface dislocations present on one side of the y-axis in the secondary array.

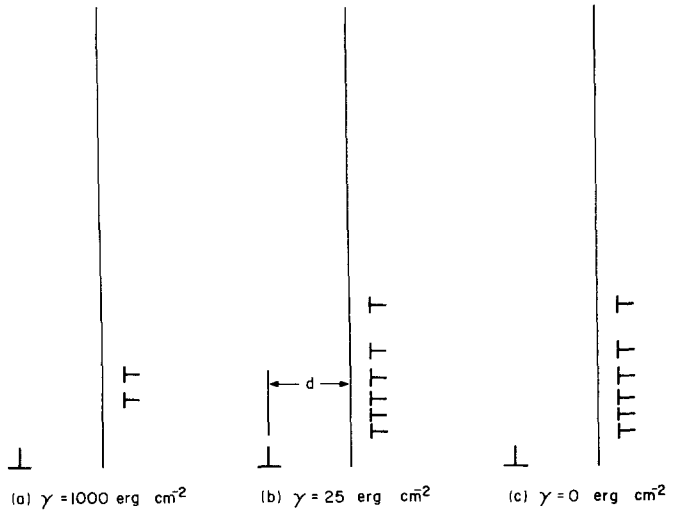

Figure 24 Dislocation configuration of the secondary array on the surface of a semi-infinite solid containing a dislocation with Burgers vector perpendicular to the surface. $d = 10$ Å from the surface.

locations is shown in Fig. 23 as a function of the surface energy γ. The energy of the configuration E_T and the associated number of surface dislocations in the array, N_s, are indicated at each arrow on the curve. It is seen that a surface energy of $1000\,\text{erg}\,\text{cm}^{-2}$ eliminates almost all of the surface dislocations except two. The dislocation configuration is shown in Fig. 24 for three values of γ. It is seen that with increasing γ, the surface dislocations become eliminated and move towards the point of maximum interaction, $y = d$ on the surface. The spreading of the surface array of dislocations is also greatly reduced as illustrated by the dislocation configuration for $\gamma = 1000\,\text{erg}\,\text{cm}^{-2}$. It is also seen that the energy contribution for relaxation of the surface is only of the order of $10^{-5}\,\text{erg}\,\text{cm}^{-2}$ from the secondary array, while it is of the order of $10^{-3}\,\text{erg}\,\text{cm}^{-2}$ from the primary array. It is for this reason that the second surface array is considered to be of secondary importance.

The discrete dislocation analysis can be carried out for the primary array for a lattice dislocation with Burgers vector parallel to the free surface

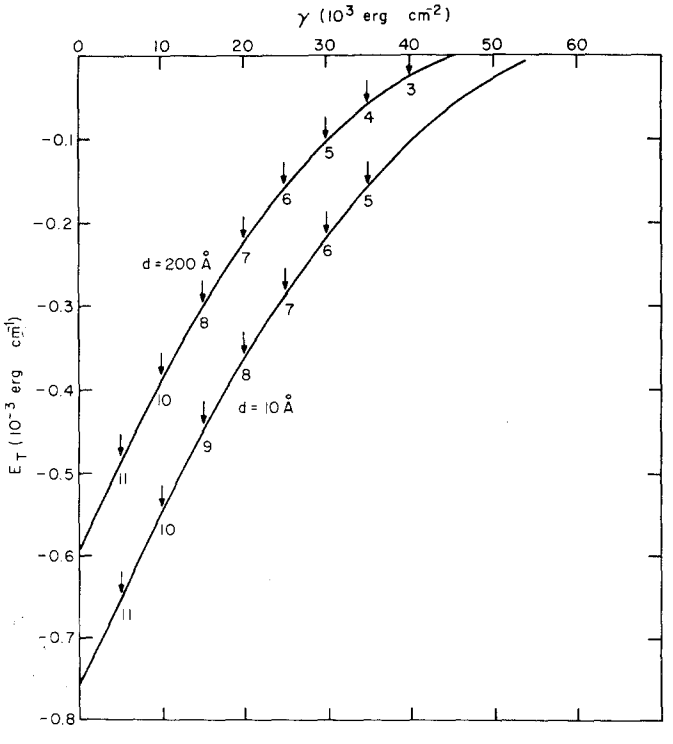

Figure 25 E_T, the total energy of the configuration obtained by the minimization procedure using the discrete dislocation method. The arrows and the associated numbers indicate the number of surface dislocations present on one side of the y-axis in the primary array.

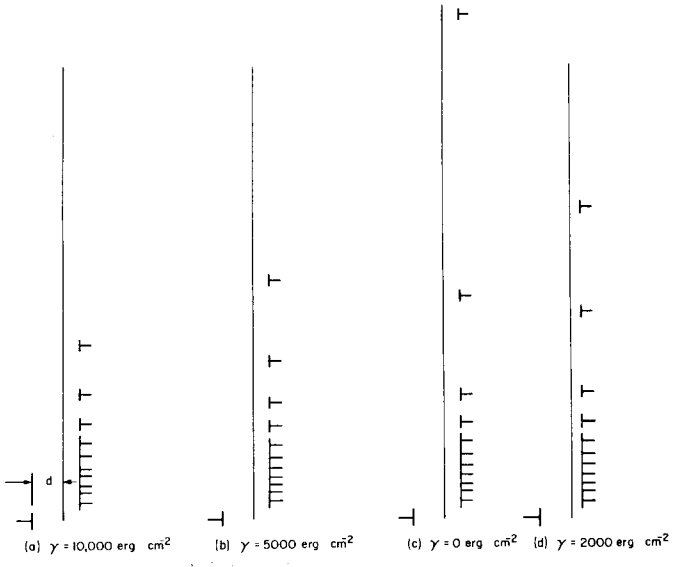

Figure 26 Dislocation configuration of the primary array on the surface of a semi-infinite solid containing a dislocation with Burgers vector parallel to the surface. $d = 10$ Å from the surface. For $\gamma = 0$, one of the dislocations in the surface array situated away could not be shown.

when the interaction energy terms in Equation 14 are replaced by the appropriate terms. The results of the minimization of the E_T to determine the positions of the dislocations are shown in Fig. 25 as a function of γ for two values of d. The energy of the configuration and the associated number of dislocations in the surface array are shown by arrows on each curve. It is seen that the primary surface array can be eliminated completely only with very high surface energy. The dislocation configurations obtained after minimization of the energy of the configuration are shown in Fig. 26 for various values of γ. It is seen that the spreading of the surface array is much greater in comparison to the primary array near a lattice dislocation with Burgers vector perpendicular to the surface. It is also to be noted that the surface array does not move towards the $y = 0$ point because the interaction energy is not a maximum there. It is seen that the maximum number of dislocations is found near $y = d$. The secondary surface array for the lattice dislocation with Burgers vector parallel to the free surface behaves in the same way as that near a lattice dislocation with Burgers vector perpendicular to the free surface. Therefore, the analysis and results are not presented here separately. The results shown in Figs. 23 and 24 apply to the secondary array with Burgers vector parallel to the free surface. It should also be mentioned that the method of discrete dislocations gives results to any accuracy required provided the Burgers vector of the surface array is chosen sufficiently small, and correspondingly the number of dislocations in the surface array will be large. While the method of continuously distributed dislocations gives results which are very exact, the discrete dislocation method has the advantage that it can be adopted with ease to complex geometries and finite bodies where the effect of surface energy is equally important. It is seen from the results obtained by the discrete dislocations method, that they are in good agreement with the results obtained by the continuous distribution method.

5. Further applications of the present results

It has been relatively simple to take into account the effect of surface energy because the surface array directly gives the ledge area and the additional surface energy associated with it. Thus, the surface dislocation method has the added advantage that it can analyse all the surface phenomena associated with the relaxation of the surfaces under either an external stress source or an internal stress source as illustrated here. Other methods, namely the Green's function technique and the image dislocation method lack this advantage, unless modified. The analysis of the effect of surface energy on the surface boundary

conditions using the surface dislocation model is a good illustration of the superiority of the surface dislocation model over the other methods.

The present results also indicate that the free surface boundary conditions used in classical linear elasticity are not strictly valid since the effect of surface energy will be to eliminate the surface arrays and thus introduce stresses on the surface of the solid. Since the surface arrays present make certain of the stresses vanish on a part of the surface, the remaining part of the surface will be made susceptible to environmental interaction and thus introduces non-uniformily stressed regions. The effect of the surface energy on the surface boundary conditions is thus very important and should be considered in many phenomena.

Many physical phenomena depend on the total amount of surface area exposed as well as on the surface morphology. The nucleation of any microscopic process starts on the surface of a solid where extra ledge surface is present due to internal sources of stress, namely dislocations. A particular example is catalysis. It is well known that chemical reactions depend strongly on the form of the surface. An array or group of dislocations near the surface gives rise to a large ledge area modified by the surface energy in the form illustrated for a single dislocation. The effect of the surface conditions due to internal sources of stress could modify the particular reaction phenomena to varying degrees. In particular, the present study shows that the surface morphology due to internal sources of stress arising from dislocations is a very important consideration. The surface dislocation approach in analysing such phenomena is shown to be a very powerful method.

6. Summary and conclusions

The method of continuously distributed dislocations and the method of discrete dislocations are used to study in detail the effect of surface energy on the surface boundary conditions of a solid containing an edge dislocation. Two orientations of dislocations, with Burgers vector perpendicular to the surface and parallel to the surface are considered and the primary and secondary arrays of dislocations are determined in each case taking into account the effect of surface energy. The dislocation distribution functions representing the surface arrays are determined exactly. The minimization of the energy of the configuration has been used to determine the spread of the surface array on the surface. The effect of surface energy is to eliminate the surface arrays, while the effect of the stress field of the dislocation is to retain the surface arrays. It has been found that very high values of surface energy are required to eliminate the primary arrays completely, but the secondary surface arrays are eliminated almost completely with very small values of surface energy. In general, for normal values of surface energy, the secondary surface array is almost completely eliminated. The results of the discrete dislocation method are in close agreement with those of the continuous distribution method. While the discrete dislocation method is not as exact as the mathematically exact continuous distribution method, it has the advantage that it can be employed in situations of complex geometries where the mathematical analysis may become prohibitively complex. Thus, the discrete dislocation method can be adapted to any situation.

It has been shown that the surface dislocation method enabled an analysis to be made of the effect of surface energy on the surface boundary conditions of the internally stressed solid. Thus, the surface dislocation method is superior to the other classical methods of linear elasticity and dislocation theory and thus, may be employed in order to study the surface relaxation phenomena.

Acknowledgements

The computer time for this project was supported in full through the facilities of the Computer Science Centre of the University of Maryland. Financial support for the present study was provided by the US Department of Energy under Contract No. AT-(40-1)-3935.

References

1. F. R. N. NABARRO, *Adv. Phys.* **1** (1952) 269.
2. J. M. BURGERS, *Proc. Kon. Ned. Akad. Wetenschap.* **42** (1939) 293.
3. J. P. HIRTH and J. LOTHE, "Theory of Dislocations", (McGraw Hill, New York, 1968).
4. T. MURA, in "Advances in Materials Research", edited by H. Herman (Interscience, New York, 1968) pp. 3, 1.
5. A. K. HEAD, *Proc. Phys. Soc. (London)* **B66** (1953) 793.

6. J. WEERTMAN and J. R. WEERTMAN, "Elementary Dislocation Theory", edited by M. E. Fine (Macmillan, New York, 1964).
7. K. JAGANNADHAM and M. J. MARCINKOWSKI, *Phys. Stat. Sol.* **50** (1978) 293.
8. *Idem, Mater. Sci. Eng.* (to be published).
9. *Idem, J. Apply. Phys.* (submitted).
10. J. D. ESHELBY, *Phil. Mag.* **40** (1949) 903.
11. M. J. MARCINKOWSKI, in "Advances in Materials Research", edited by H. Herman, (Wiley, New York, 1971) pp. 5, 445.
12. M. J. MARCINKOWSKI, *Acta Mech.* (to be published).
13. *Idem, ibid* (to be published).
14. N. I. MUSKHELISHVILI, "Singular Integral Equations" (Noordhodd, Gröningen, Netherlands, 1953).

Received 8 March and accepted 18 September 1978.